

# Outline

Diffusion tensor imaging (DTI) is an advanced magnetic resonance technique which has opened a new avenue to assess the relationship between brain function, neuroanatomy and pathology. Apart from monitoring major diseases, such as stroke, multiple sclerosis and Alzheimer's disease on the basis of several quantities describing ultrastructural tissue properties, clinical neuroscience greatly benefits from the possibility to non-invasively map detailed subsystems and circuits interconnecting neuronal centres. The latter application is known as fiber tracking, also referred to as tractography. With its integrative capacity for the build-up of atlases and, in conjunction with functional imaging for the investigation of networking regions, fiber tracking allows for a better understanding of the human brain.

Biophysically, DTI and in particular fiber tracking relies on the strongly anisotropic diffusion of water molecules in cerebral white matter. Using special acquisition schemes, the local process can be assessed by calculating a  $(3 \times 3)$ -dimensional diffusion tensor for each volume element (voxel) of the brain. The spatial tensor field provides information on the extent of anisotropy and on local fiber orientation. Importantly, the typical size of an imaging voxel (between  $1 \times 1 \times 1$  and  $3 \times 3 \times 3 \text{ mm}^3$ ) largely exceeds the scale of the reflected microscopical diffusion processes on the cellular level. The limited spatial resolution of diffusion images leads to partial volume effects with a mixture of directionalities within one voxel and consequently to ambiguity for fiber tracking algorithms. Various sources of noise inherent to DTI data acquisition also contribute to the uncertainties in the rough estimate of the average fiber orientation in space. Therefore, regularization methods that are needed to denoise diffusion weighted images and/or tensor data should make adequate use of neighbourhood information to utmostly preserve the underlying

anatomical information. Also other applications such as voxelwise statistical analysis of maps of diffusion tensor derivatives and spatial normalisation algorithms would largely benefit from edge preserving interpolation tools.

This application field poses considerable statistical and numerical challenges. In particular, the massive dimension of realistic data sets does represent a computational burden if not broken down to voxelwise or sequential operations. To date, numerous concepts of denoising have been suggested at different stages of DTI data processing, ranging from anisotropic kernel methods and other adaptive filtering schemes to iterative or multilevel procedures. These methods pursue the preservation of detailed anatomical structures and the adequate consideration of the errors that follow a Rician distribution after Fourier transformation. Efforts have been spent on the issue of tensor estimation with respect to the positive definiteness and robustness as well as non-linearity of the model and mixing distributions. In view of fiber tracking, polynomial interpolation techniques and basis function approaches are in use. So far, not more than smoothing and interpolation have been melted into one processing step in order to reduce error propagation. Therefore, the main goal of this thesis is to offer a unified framework for DTI data processing with the outlook to improve fiber tracking.

To facilitate the understanding to the reader unfamiliar with the given technology, **Chapter 1** provides fundamental background information on magnetic resonance tomography and explains the biophysical principles of DTI. Apart from data acquisition the use of derived quantities is illuminated. In **Chapter 2**, the impact of noise on data quality is investigated using the non-parametric bootstrap method. The procedure allows to quantify statistical uncertainties of DTI data and derived characteristics in dependence on thermal noise and subject motion, either artificially increased or reduced by spatial smoothing and the use of a vacuum device. Also, effects of gender and age are addressed as potential confounds in group comparison studies. The extended use of bootstrap as a tool for quality evaluation of tensor derived metrics and reconstructed fiber bundles is reviewed. **Chapter 3** deals with the three-stage processing pipeline towards tractography. For the purpose of unified estimation, regularization and interpolating of the diffusion tensor field, a space-varying coefficients model (SVCM) is developed on the basis of penalized B-spline basis functions. The joint modelling of the separate regression

equations naturally takes into account spatial correlation by the use of basis functions which also allow the tensor estimation at any arbitrary point in space. Yet, a naive one-to-one implementation of the model formula is limited by the relatively large dimension of realistic data sets which typically contains multiple images of  $(128 \times 128 \times 24)$  voxels. Tackling the problem of memory allocation, sparsity of the involved matrices of tensor product B-splines and difference penalties had to be incorporated. In addition, a sequential smoothing variant is considered as efficient alternative. A simulation study compares the novel concept to standard procedures. The chapter closes with a tutorial on the corresponding open-source software comprising both variants of the novel concept and toy data. In **Chapter 4**, wavelets are explored for their utility in DTI data processing. One- and two-dimensional examples serve for the derivation of the wavelet theory and the illustration of the multiscale property. A wavelet filter which accounts for the positive definiteness of diffusion tensors is established and examined for adaptive post-denoising of the 3d tensor field estimated on a voxel-by-voxel basis from synthetic and experimental data. Apart from replacing Gaussian kernel smoothing, wavelets could be used to substitute the B-spline basis functions in an SVCM. A proposal is made how this could be accomplished. In **Chapter 5**, the SVCM for simultaneous tensor estimation, smoothing and interpolation is finally linked to an existing tractography algorithm which is sketched in brief. Examples of reconstructed fiber bundles of the human brain are visualized and discussed. To conclude, an outlook is given on the exchange of B-spline with wavelet basis functions.

This thesis initially originates from a cooperation with the research group of nuclear magnetic resonance at the Max Planck Institute of Psychiatry, Munich. It directly picks up the work by Christoff Gössl, also developed within the project *Spatial Statistics* of the Collaborative Research Center *Statistical Analysis of Discrete Structures*. Financial support was provided by the German Science Foundation (D. F. G.).



# 1 Introduction to Magnetic Resonance Imaging (MRI)

Nuclear magnetic resonance imaging deserves to be called a milestone in innovating diagnostic medicine. The chemist Paul C. Lauterbur and the physicist Sir Peter Mansfield contributed the relevant findings throughout the 1970s and were awarded the Nobel Prize in Medicine and Physiology in 2003. Medical engineering promoted the realization and continues the improvement of the magnetic resonance tomograph (Fig. 1.1) which is basically equipped with a strong magnet, a radio frequency transmitter and receiver, and gradient coils.



*Figure 1.1: Patient positioned in an MR scanner for image acquisition of the human brain.*

The technique exploits the interaction of radio frequency pulses, a strong magnetic field and body tissue. It comes with considerable advantages, in particular, when compared to conventional, X-ray imaging techniques: The use of magnet resonance (MR) principles allows the generation of extremely detailed 3d images from inside the human body in a non-invasive way, without technical or health risk and without exposure to high-energy radiation. As further benefit, imaging contrasts can be adapted in a flexible manner, rendering MRI a powerful instrument to visualize and to quantify a large range of tissue properties down to a microscopic scale.

In clinical practice, MRI enables disease diagnosis and monitoring. It offers techniques that go beyond traditional imaging to show functional aspects of the investigated tissue. Diffusion tensor imaging (DTI) is one of the more advanced techniques that entered the clinical field in the 1980s. It has proven effective in studying aging processes (Moseley, 2002) and a range of neurological disorders, comprising stroke (Sotak, 2002), brain tumors, focal epilepsy, Alzheimer disease, and inflammatory diseases such as Multiple Sclerosis (Horsfield and Jones, 2002). A very promising technique for neuroscience and also clinical applications is fiber tracking, i. e. the visualization of neural fiber tracts in the brain that connect different brain regions with each other and with the myelon. This may become increasingly important in neurosurgery, when e. g. the effect of brain tumors on neighboring fiber tracts is assessed for planning of surgery (Arfanakis et al., 2006; Schonberg et al., 2006). Fiber tracking also represents a final application field of the statistical methods developed in this work (Chapter 5). In contrast, physicochemical properties such as metabolite information are generally assessed by MR spectroscopy. Moreover, functional MR imaging (fMRI), which has entered the field of neuroimaging in about 1992, has greatly advanced the understanding of normal and abnormal brain function, including sensorimotor functions but also cognitive and emotional processes. A core concept in fMRI analysis is the functional connectivity, i. e. the interaction of brain regions during a task.

At this point, DTI based tractography has become an important tool to demonstrate the real underlying anatomical connectivity. Further research aims at localizing networks of brain regions that are affected by pharmacological intervention, for example by antidepressive treatment. The outlook here is to identify, how pharmacons alter brain function

and to improve treatment strategies for different neuropsychiatric conditions.

This chapter is organized in two sections: first, the basics of MR physics are introduced in Section 1.1 and, second, the particular technique of DTI is explained in Section 1.2. Basic questions will be answered such as *what* is measured and *how* an image is formed. For more profound reading on both subjects, the book chapters 15 and 16 in Toga and Mazziotta (2002) can be recommended as well as the contributions in Weickert and Hagen (2006). Also, several excellent review articles provide fundamental understanding of DTI, e. g. Le Bihan (2003), Mori and Barker (1999) and Basser and Jones (2002).

## 1.1 Basic principles of MRI

Hydrogen is omni-present and one of the most frequent elements in the human body. The nucleus of a hydrogen atom consists of one single proton. Due to the intrinsic spin of the proton, the rotating positive charge results in a current which in turn induces a magnetic field. Hence, hydrogen protons have a magnetic dipole moment parallel to the rotating axis and can be considered as tiny magnetic needles that react to external magnetic fields. Under normal conditions, free proton spins are randomly orientated in space (Fig. 1.2, left). In the presence of an external magnetic field, the protons take on one of the two quantum mechanically possible energy levels, leading to parallel or antiparallel alignment with the magnetic field (Fig. 1.2, right). This state is called equilibrium. With increasing field strength, fewer protons are strong enough to align against the magnetic field. There is a small excess of spins aligned parallel to the external field yielding an overall net magnetization. In an MR scanning device, this magnetization vector points along the human body and is therefore referred to as longitudinal magnetization,  $M_z$ .

Yet, the protons do not comply statically with the lines of magnetic flux as suggested by Fig. 1.2, but precess, similar to tops, around the external field direction at an angular frequency. This frequency is called Larmor frequency and depends on the atom specific gyromagnetic ratio and the strength of the external magnetic field. At a magnetic field strength of 1.5 Tesla (T), commonly found in clinical MR scanners, the hydrogen spins precess at 63.9 MHz. The protons can change their spin direction if energy is added by

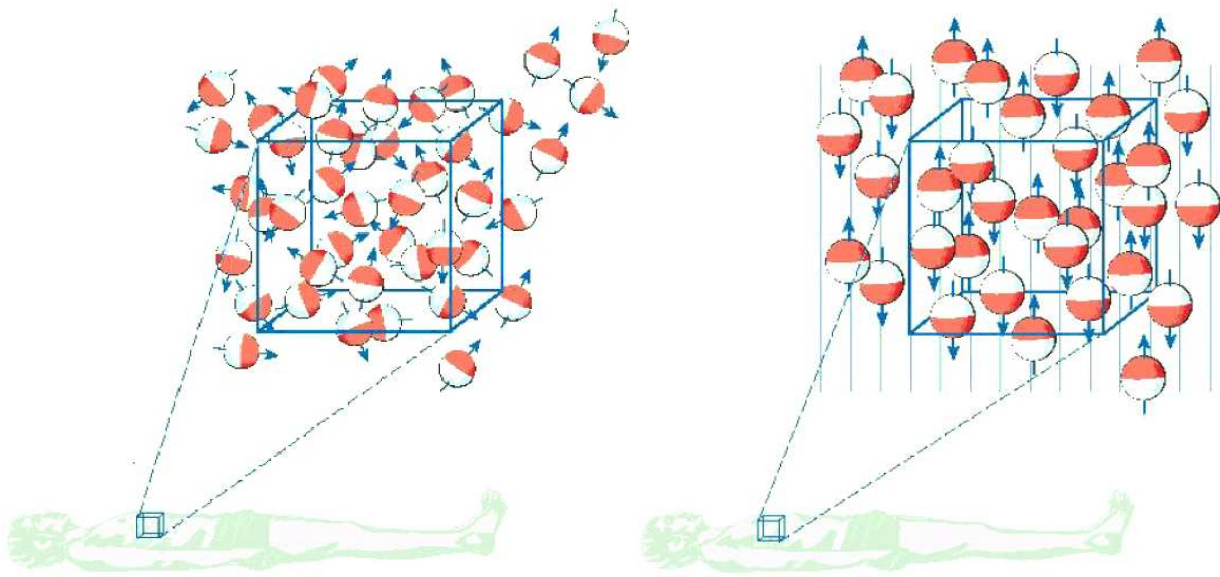


*Figure 1.2: Protons are naturally in a disordered state (left), but can be aligned with an external magnetic field (right).*

transmission of a suitable electromagnetic radio-frequency (RF) pulse. The RF needs to match the Larmor frequency of the magnetic spins so that the spins can couple to the magnetic component of the RF field (resonance condition) and exchange energy. The resulting spin distortion is a nuclear magnetic resonance phenomenon, giving the technique its name. After energy absorption the nuclei release this energy and return to their initial state of equilibrium. The emitted energy establishes the MR signal that is a function of contrast determining tissue parameters (proton density, relaxation times  $T_1$  and  $T_2$ ) and the machine parameters (time to echo ( $TE$ ) and time to repetition ( $TR$ )), which will be explained in the following.

The most common pulse sequences employed in MR imaging are spin echo sequences. A  $90^\circ$  RF pulse is applied for spin excitation, i. e. deflecting the magnetic moment by  $90^\circ$  from the direction of the external field. As a consequence, the longitudinal magnetization is rotated into the  $xy$ -plane. Indeed, the excitation pulse causes the protons to precess in-phase, generating a transversal magnetization  $M_{xy}$ . Since the transversal magnetic moment also appears to be rotating at Larmor frequency, an MR signal voltage is induced and can be measured by a receiver station. After the shortly lasting RF excitation pulse, the transversal magnetization decreases and also the corresponding signal intensity. The



free induced signal decay (FID) occurs because individual spins lose their coherence and dephase with time due to magnetic interaction among each other. Thus, the dephasing mechanism is characterized by the spin-spin relaxation time, denoted by  $T_2$ . For the purpose of signal detection, a  $180^\circ$  refocusing RF pulse is applied after duration  $\tau$  of the initial  $90^\circ$  excitation pulse, causing the spins to reverse their rotation direction. After  $2\tau = TE$ , the time to echo, the faster, now counterrotating spins have caught up with the slower ones and the spin echo appears in dependence on the surrounding tissue properties. For example, protons are very mobile in water and have less opportunity to exchange energy. Therefore, the amount of transverse magnetization relaxes more slowly than e. g. in fat. Water gives a stronger signal and appears brighter on the image than fat. Nevertheless, there will be some intensity loss due to local field inhomogeneities.

The recovery of the longitudinal magnetization occurs with the  $T_1$  relaxation time and typically at a much slower rate than the  $T_2$  decay. The recovery process is driven by energy exchange of the spins with their surroundings and is therefore also named spin-lattice relaxation. Protons can efficiently interact with fatty acids (short  $T_1$ ) whereas in liquids protons move too fast for notable energy transfer (long  $T_1$ ). Depending on the kind of sequence used, this results in varying image brightness.

In summary, the signal intensity of the echo in a spin echo sequence is related to the square of  $M_{xy}$ , given by:

$$M_{xy}(t = TE) = M_{xy}(0) (1 - \exp(-TR/T_1)) \exp(-TE/T_2), \quad (1.1)$$

where  $M_{xy}(0)$  denotes the transversal magnetization right after the first excitation which is equal to the longitudinal magnetization  $M_z$  at time  $t = 0$  and, thus, proportional to the proton density. After later excitations, the signal intensity of the echo is essentially determined by the first two factors, where the dependency on  $TR$  describes the longitudinal magnetization rebuilt since the preceeding  $90^\circ$  pulse. For the moment being, it suffices to know that  $TR$  denotes the time interval before the whole pulse sequence is repeated. According to Eq. (1.1), the MR signal consists of three factors that can be down-regulated or enhanced by control of  $TE$  and  $TR$ . Different image contrasts can be obtained, named proton density weighting (short  $TE$ : 20 ms, long  $TR$ ),  $T_1$  weighting (short  $TE$ : 10–20 ms, short  $TR$ : 300–600 ms), and  $T_2$  weighting (long  $TE$ :  $> 60$  ms, long  $TR$ :  $> 1600$  ms). Figure 1.3 gives an impression of these basic MRI modalities by means of an axial slice